THE UNIVERSITY of EDINBURGH

Edinburgh Research Explorer

An investigation of the effects of wind-induced inclination on floating wind turbine dynamics: heave plate excursion

Citation for published version:
Antonutti, R, Peyrard, C, Johanning, L, Ingram, D & Incecik, A 2014, 'An investigation of the effects of wind-induced inclination on floating wind turbine dynamics: heave plate excursion', *Ocean Engineering*, vol. 91, pp. 208-217. https://doi.org/10.1016/j.oceaneng.2014.09.008

Digital Object Identifier (DOI):
10.1016/j.oceaneng.2014.09.008

Link:
Link to publication record in Edinburgh Research Explorer

Document Version:
Early version, also known as pre-print

Published In:
Ocean Engineering

General rights
Copyright for the publications made accessible via the Edinburgh Research Explorer is retained by the author(s) and / or other copyright owners and it is a condition of accessing these publications that users recognise and abide by the legal requirements associated with these rights.

Take down policy
The University of Edinburgh has made every reasonable effort to ensure that Edinburgh Research Explorer content complies with UK legislation. If you believe that the public display of this file breaches copyright please contact openaccess@ed.ac.uk providing details, and we will remove access to the work immediately and investigate your claim.

Download date: 05. May. 2023

An investigation of the effects of wind-induced inclination on floating wind turbine dynamics: heave plate excursion

Raffaello Antonutti[a,b,c,*], Christophe Peyrard[a,c], Lars Johanning[e,b], David Ingram[d,b]

[a] *EDF R&D - Electricité de France Research and Development, 6 quai Watier, 78400 Chatou, France*
[b] *Industrial Doctoral Centre for Offshore Renewable Energy, The University of Edinburgh, King's Buildings, Edinburgh EH9 3JL, UK*
[c] *Saint-Venant Hydraulics Laboratory, Université Paris-Est, 6 quai Watier, 78400 Chatou, France*
[d] *Institute for Energy Systems, School of Engineering, The University of Edinburgh, King's Buildings, Edinburgh EH9 3JL, UK*
[e] *College of Engineering, Mathematics and Physical Science, Renewable Energy Research Group, University of Exeter, Penryn Campus, Penryn TR10 9EZ, UK*

Abstract

A current trend in offshore wind is the quest for exploitation of ever deeper water sites. At depths between 50 m and 100 m a promising substructure is the column-stabilised semi-submersible floating type. This solution is currently being tested at full scale at the WindFloat and Fukushima Forward demonstrator sites in Portugal and Japan respectively. The semi-sub design class frequently adopts passive motion control devices based on the water entrapment principle, such as heave plates, tanks, and skirts. Whilst effective for small inclinations, these can underperform when the structure is inclined as a result of wind loading. This study examines the alteration of potential hydrodynamics due to wind-induced trim (geometric non-linearity) and its impact on the floating wind turbine's wave response with focus on heave plate performance. Firstly it is shown by using the boundary element approach that wind trim affects wave loading in the ocean wave band between 5 s and 15 s, and introduces hydrodynamic coupling typical of non-symmetric hulls. These features are incorporated in frequency-domain dynamic response analysis to demonstrate that said hydrodynamic effects bear a significant impact on the turbine's wave response. Accounting of heave plate excursion effects improves the assessment of the seaworthiness of floating wind turbine concepts, potentially leading to new design constraints.

Keywords: floating wind turbine, semi-submersible, heave plate, water entrapment, inclination, tilt

1. Introduction

Going afloat is deemed to be one of the principal innovations to impact the offshore wind market in the next years, enabling expansion to deep water areas where bathymetry exceeds 50 m (EWEA, 2013). Numerous countries worldwide hold most of their offshore wind potential in deep water, but so far only a handful have hosted utility-scale machine deployment. Statoil of Norway has commissioned the first operating MW-class floating demonstrator, Hywind, in 2009 (Stiesdal, 2009). Portugal has followed by hosting Principle Power's WindFloat prototype (Figure 1), and more recently two Japanese consortia have successfully installed floating test units off Goto city (Figure 2) and Fukushima (see Hitachi, 2014; Main(e) IC, 2013). All commissioned large scale prototypes adopt turbines of about 2 MW capacity, mounted either on spar or semi-submersible type substructures. The ongoing industrialisation initiatives are seeking to extend the FWT (floating wind turbine) design envelope with the use of tension leg type platforms (see Scott, 2012), vertical axis turbine technology (see IWES, 2014; Nénuphar, 2012), and by increasing turbine size.

1.1. Semi-submersible platform

Semi-submersible, column-stabilised platforms are currently investigated as a low-draft, easy-handling FWT substructure solution. Unlike spars and tension-leg floaters, they count on widely spaced columns of large waterplane area to insure the stability necessary to counter wind-induced overturning moment. Normally these columns are interconnected by lattice frames or pontoons.

Most proposed semi-sub designs feature water entrapment plates or tanks located at column foot which provide extra added mass, wave damping, and drag, as well as buoyancy far removed from wave excitation. The resulting heave added mass and hydrodynamic inertia in roll and pitch can be very significant, and often reach the same order of magnitude of the FWT's own structural inertias. This effect is fundamental in order to shift natural periods beyond the wave range while preserving sufficient stability and simultaneously limiting floater size.

Water entrapment devices should be used with caution by platform designers, because they can also aggravate wave loading. In fact they extend the structure's wetted surface receiving fluid loads, giving raise to additional vertical excitation. Extra horizontal excitation on nearby vertical members is also possible due to perturbation of the diffrac-

*Corresponding author

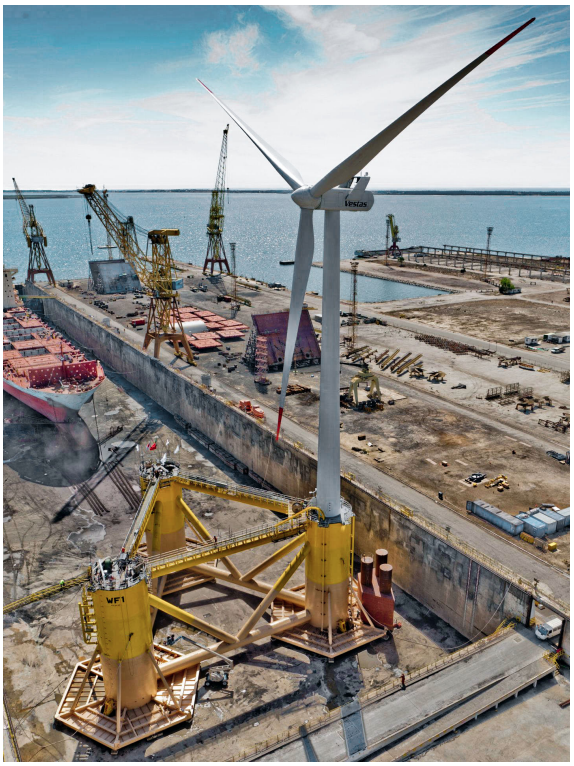

Figure 1: WindFloat assembly in the Mitrena Shipyard near Lisbon. Water entrapment plates are visible at the bottom of the semi-submersible platform's columns. Source: Cermelli (2014), photo courtesy of Principle Power Inc.

Figure 2: Haen-kaze, the 2 MW floating wind turbine demonstrator sited off Goto in Japan. Photo courtesy of David Ingram.

tion pattern, and to enhanced wave run-up. Such adverse effects, observable if the plates have a limited submergence compared to their size, have been observed experimentally by Cermelli and Roddier (2005) on a low-draft offshore platform model. Another experimental study by Philippe et al. (2013b) has shown pitch motion amplification on a FWT, which was orientatively attributed to heave plate excursion.

1.2. Floating wind turbine dynamics

FWT dynamic response under the action of met-ocean loads has been extensively investigated in recent years, leading to development of coupled models able to treat simultaneous hydrostatic, hydrodynamic, and aerodynamic loading on the structure, taking into account its deformability in certain cases. Most work to date adopts a fully linear approach to potential wave hydrodynamics assuming small amplitude waves and motion about the unexcited configuration - see for example Karimirad and Moan (2012), Jeon et al. (2013), Sethuraman and Venugopal (2013), and Wang and Sweetman (2013). A few studies implement updated wetted surface meshing to incorporate the geometric non-linearity due to quasi-steady displacement of a FWT under the wind's action; this allows to integrate the dynamic pressure associated to the Froude-Krylov, diffraction, and radiation problems over the displaced wetted surface, effectively re-linearising potential hydrodynamics about a more representative mean position. In particular, Philippe et al. (2013a) actualise the mesh of a circular barge supporting a FWT to characterise its motion under simultaneous wind and wave loading; Philippe (2012) and Philippe et al. (2013b) re-mesh a semi-sub FWT platform hull for similar purposes, although removing the water entrapment plates from the potential flow problem. Inclinations matter in this context: current generation FWT concepts can experience mean wind-induced trimming in excess of 5 ° in certain circumstances (see Courbois, 2013; Hujis et al., 2013; Philippe et al., 2013b), especially when floater size - and therefore stability - is reduced to seek material efficiency.
In this work it is shown that capturing the geometric non-linearity due to large-angle inclinations may be important in predicting the motion of a semi-sub FWT under simultaneous wind and wave loading, and that water entrapment appendices play a key role in this respect. A mesh-updated approach based on the linear potential method is used to provide a first-tier account of this non-linearity.

2. Excursion effects on water entrapment plate hydrodynamics

The focus of this section is the effect of varying the submergence of thin horizontal structures on their diffraction/radiation loading, to capture the key features influencing heave plate behaviour. A review of the submerged plate problem is first presented, and then a more

applied case study is proposed, where a FWT column with bottom-mounted heave plate is studied in its vertical excursion. Last, the problem is formulated globally for a trimming semi-submersible platform.

2.1. Review of submerged horizontal plate problem

Offshore oil & gas structure researchers have in the past investigated water entrapment device behaviour for motion control of deep draft floating facilities. Studies are available which look at bottom plate forces (Lake et al., 2000; Thiagarajan et al., 2002) and local flow separation (Tao and Cai, 2004; Tao et al., 2007). None of these addresses the alteration of the diffraction/radiation problem of a plate of varying submergence. Underwater horizontal plates have also been extensively studied in the field of coastal engineering - a general account of the material published up to 2002 is given by Yu (2002). Large flat structures are regarded as a potential breakwater solution exploiting fluid-fluid interaction (Yu, 2002), but also as wave focussing devices for wave energy extraction purposes (McIver, 1985); the issue of variable submergence is largely covered in the field. Next follows a scrutiny of the relevant coastal engineering and fluid mechanics research, noting that a heave plate, although small compared to a breakwater, will be exposed to similar surface proximity effects if brought close enough to the still water level.
The wave diffraction problem of a thick plate has been addressed by Zheng et al. (2007) under linear approximation and by Kojima et al. (1994) up to the II order, while that of a thin plate is discussed in Porter (2014). Its formulation for an arbitrarily shaped, submerged cylinder is also proposed by Vada (1987). The linear wave radiation problem of a heaving horizontal disc has been studied in Martin and Farina (1997) and in Porter (2014). The latter study treats an infinitely long flat plate as well, while Zheng et al. (2007) analyse wave radiation resulting from the oscillation of a thick rectangular pontoon; this work also shows that the wave forces and coefficients obtained with the BEM (boundary element method) approach fit well the results of the popular approach based on eigenfunction expansion matching.
The recapitulative messages for our use deriving from the above review are:

- The submergence of a plate- or pontoon-shaped structure can strongly influence first and higher order wave forces and hydrodynamic coefficients (see example in Figure 3).
- The behaviour of the first order quantities above consists in increased response as submergence is reduced, with the partial exception of added mass.
- First order forces prevail if submergence is sufficiently large compared to the horizontal size of the structure. At very small submergence (one order of magnitude below structure size or less), non-linear effects dominate and numerical resolution becomes increasingly difficult.
- Most modelling methods are based on potential flow. The majority of them subdivide the fluid domain and match the resulting eigensolutions of the Laplace equation to deduce the potential.
- This method yields good agreement with the experimental results obtained in terms of wave forces, given that viscous effects be superposed using calibrated drag coefficients.
- At first order, the results of the above models are virtually equivalent to those found with the BEM approach.

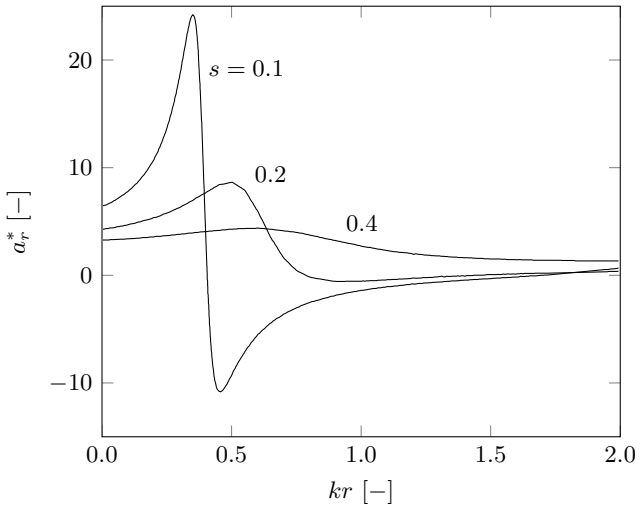

Figure 3: Variation of the non-dimensional heave added mass $a_r^* = a_r/(\rho r^3)$ of a thin horizontal disc in infinitely deep water, depending on its submergence $s = d/r$. Disc radius and draft are denoted r and d respectively, a_r is the dimensional added mass and ρ the fluid's density. $k = \omega^2/g$ denotes the wave number. Reported from Martin and Farina (1997).

The wave-plate interaction problem is rendered complex by effects of more difficult treatment such as wave trapping (Linton and Evans, 1991; Parsons and Martin, 1995), and other non-linear phenomena such as wave decomposition (Kojima et al., 1990) and breaking (Yu et al., 1995) over the plate's topside, occurring when wavelength and plate extension are large enough compared to submergence.
The studies mentioned above neglect or superpose viscous hydrodynamic effects. The complete representation of viscous wave flow over a submerged plate has been attempted by Yu and Dong (2001) using a finite volume method.
This knowledge can now be reconducted into FWT hydrodynamics, to better characterise the wave forces acting on a low draft structure fit with bottom plates.

2.2. Methodology

In this study potential fluid-structure interaction analysis is limited to first order. Wave forces and hydrodynamic coefficients are obtained numerically via Nemoh, a

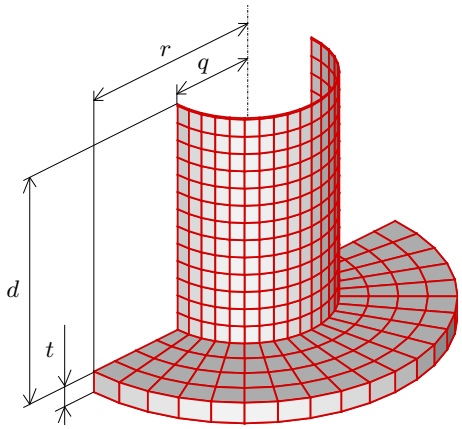

Figure 4: Mesh of modified Dutch Tri-floater column at baseline draft. Only half the structure is represented since the BEM solver can exploit planar symmetry to reduce problem size. Quote q denotes the column's radius, r the heave plate's radius, t its thickness, and d the depth of plate topside below the free surface.

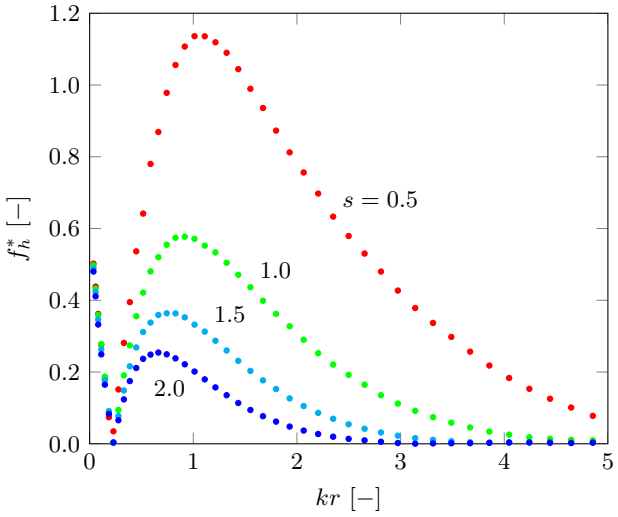

Figure 5: Variation of non-dimensional heave force $f_h^* = f_h/\rho g r^2$ (with f_h heave force RAO) when the column with water entrapment plate is displaced vertically in infinite water depth.

BEM diffraction/radiation solver made available by the Ecole Centrale de Nantes (see ECN, 2014). In 2.3 a surface-piercing column with bottom plate is analysed at different drafts. It follows a study of a three-column FWT floater (2.4) whose underwater mesh is re-calculated for three trim angles, with rotations occurring about the upright centre of waterplane. This is a floating platform's static pivoting centre, assumed that it behaves like a perfect vertical-walled (Scribanti) buoyant (see Journée and Massie, 2000).

2.3. Submergence sensitivity of a platform column

The considerations of 2.1 apply to water entrapment devices in that their vertical excursion impacts the forces arising from incident, diffracted, and radiated waves. An isolated axisymmetric column with attached bottom plate is taken from the modified Dutch Tri-floater concept, detailed in 2.4.1. A parametric study is here organised by varying the structure's relative submergence s and regenerating the wetted surface mesh at each draft. Relative submergence is defined as $s = d/r$, where d denotes upper plate surface depth and r (constant) plate radius (cfr. Figure 4). The remaining geometric proportions are fixed with $q/r = 4/9$ and $t/r = 1/9$. Solving the diffraction problem yields the wave excitation exerted on the structure: Figure 5 shows the variation of the heave force RAO obtained when submergence is perturbed, given an infinite water depth and a unit incident wave amplitude. It is possible to observe that smaller draft leads to increased excitation as anticipated in 2.1, conversely the vertical force RAO tends to zero for an infinite draft for any wave harmonic of finite period. This well-known effect is mostly observable at values of kr larger than the heave excitation suppression point, a range where the rapid exponential decay of wave potential affects the plate's depth range and diffraction is strongly affected by plate submergence.
Figures 6 and 7 report frequency-domain vertical added mass and wave damping coefficients respectively, depending on the wave scattering parameter kr. As expected, the column's heave radiation characteristics are also found to be affected by submergence: added mass (Figure 6) shows little alteration for $s > 1$; for $s \leq 1$ it is observed a pattern similar to what seen in Figure 3; the wave damping coefficient's behaviour (Figure 7), analogous to that of heave excitation, consists in exponential increase in a definite band as relative draft is reduced. The outputs of the radiation calculation suffer from a certain amount of numerical noise that could neither be attributed to insufficient mesh resolution nor to incomplete convergence of the matrix inversion. This especially affects the radiation damping coefficient for certain values of kr, where the size of the anomaly reaches a magnitude comparable to the signal for $s > 1.5$. In this region of high submergence, however, wave damping forces become small and hence the impact of said anomaly on FWT motion can be deemed negligible.
One can look at the surface proximity effect from a different standpoint: identifying the combined scattering parameter and submergence envelope where perturbing draft causes a significant change in wave forces. Figure 8 exemplifies this idea for column heave load: by defining the quantity $f_h^* = f_h/(\rho g r^2)$, where f_h is the heave force per unit amplitude incident wave, its derivative with respect to submergence $-df_h^*/ds$ may be used as a proxy for sensitivity to vertical excursion. This quantity, mapped against kr and s, exhibits a monotonic decrease as submergence is increased, and a maximum at $kr \approx 1.3$ for any constant submergence. The blue region on the right represents the range for which waves are so small that their vertical penetration is not sufficient to reach the depth of the heave plate; the low-valued areas to the left and towards the top of the plot are associated in turn to large-scale wave

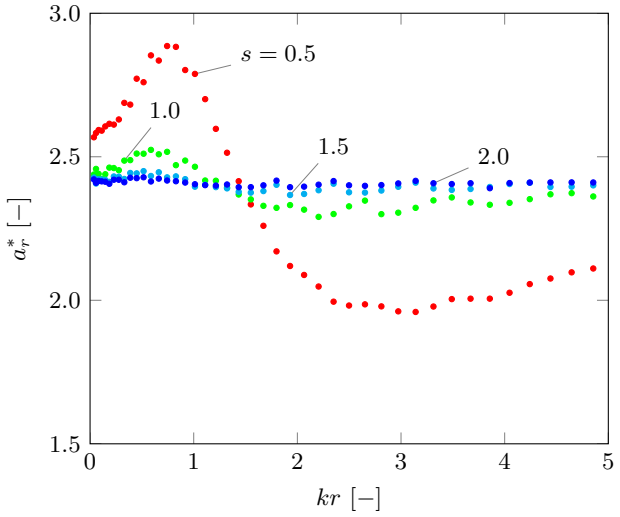

Figure 6: Non-dimensional heave added mass of column with water entrapment plate for varying submergence. For reference, the classic potential solution for the added mass of a disc of infinite submergence, available in Lamb (1945), is $a_r^* = 8/3$.

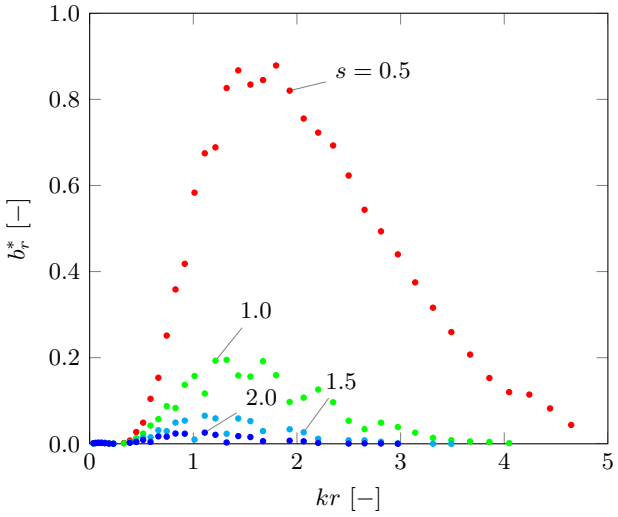

Figure 7: Non-dimensional heave wave damping coefficient $b_r^* = b_r/\rho\sqrt{gr^5}$ of column with water entrapment plate for varying submergence.

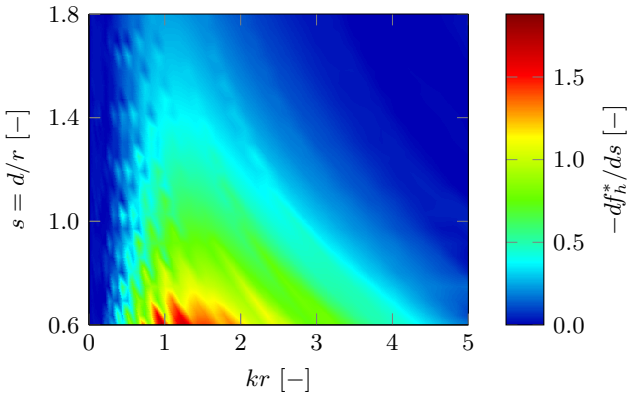

Figure 8: Vertical wave load sensitivity to submergence for a column with heave plate.

kinematics compared to structure size, and to large plate submergence: the former requires large vertical excursions to determine a change of loading regime (hence sensitivity is small), whilst the second is associated with vertical extinction of wave potential. The region of highest sensitivity sits where pronounced decay of the diffraction potential occurs just around the plate's depth.
From these simple numerical experiments one can anticipate a low-draft semi-sub platform's behaviour: when its columns lose submergence, the plates interact more strongly with surface waves, causing wave-structure interaction alterations which are most significant in a specific band. In the case of the analysed FWT concept, this region largely coincides with the dominant wave energy band.

2.4. Inclination sensitivity of a semi-sub platform

The column studied above is derived from a MW-scale FWT platform design, the Dutch Tri-floater, documented in Philippe et al. (2013b), Philippe (2012), and Courbois (2013). This has been modified as explained in 2.4.1. A perturbation analysis is conducted on platform potential hydrodynamics similar to what has been done in 2.3, only with variation of inclination in lieu of draft. The distance of the columns from the FWT's static pivoting point determines both plate excursion and rotation, causing a change in the resulting wave force patterns.

2.4.1. Platform definition

The Dutch Tri-floater is a three-column semi-sub platform concept designed to support HAWTs with a rating of about 5 MW. Its stabilising system is passive, unlike in other designs where slow-varying wind overturning moments are compensated with active ballast shifts (see Maciel, 2012). Since the original concept features thin water entrapment plates, which cause numerical problems when treated with the BEM method, it was decided to modify the floater by thickening its plates to an acceptable level; the introduction of extra submerged volume at platform bottom required contextual re-distribution of its mass in order to restore the originally intended degree of hydrostatic stability. The modified floater is shown in Figure 9, while its main geometric parameters are given in Table 1 and its mass properties in Table 2.

2.4.2. Platform tilt hydrodynamic effects

The modified Dutch Tri-floater is next subjected to isocarenic trimming of ±5 ° about the pitch axis y. Heave plates rigidly follow, undergoing the same rotation plus a vertical excursion of about ±1.7 m (aft columns) and ±3.4 m (fore column). These in turn cause plate mean submergence s to vary in the range between 0.84 and 1.60, while in the upright configuration all columns are are characterised by $s = 11/9 \approx 1.22$ (cfr. Figure 8). Actualisation

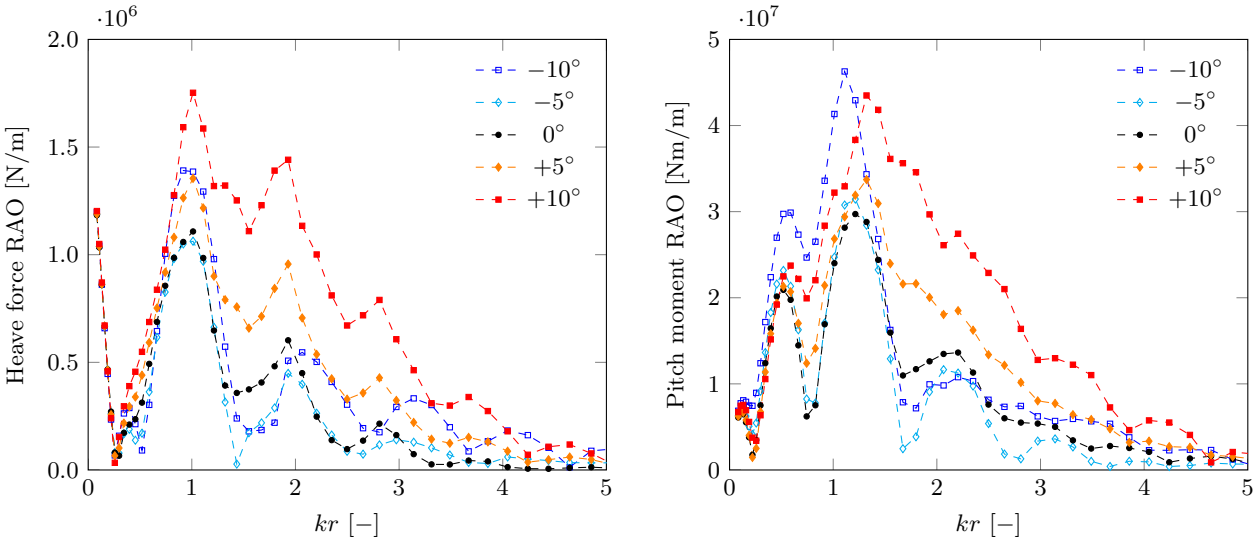

Figure 10: Inclination effects on the modified Dutch Tri-floater's heave force and pitch moment response in regular waves.

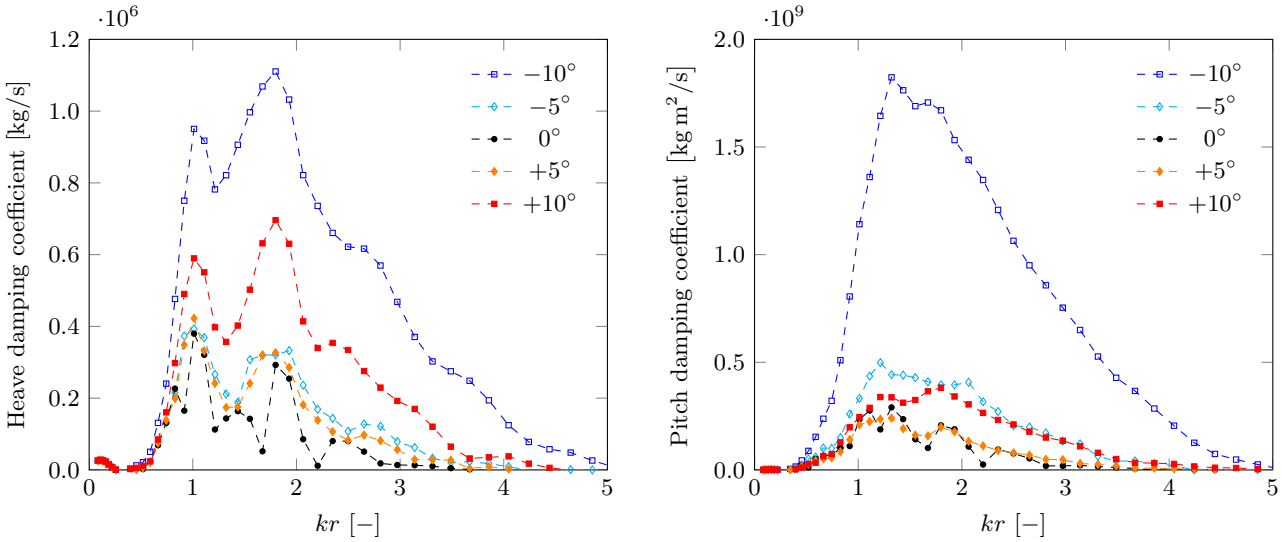

Figure 11: Inclination effects on the modified Dutch Tri-floater's heave and pitch radiation damping.

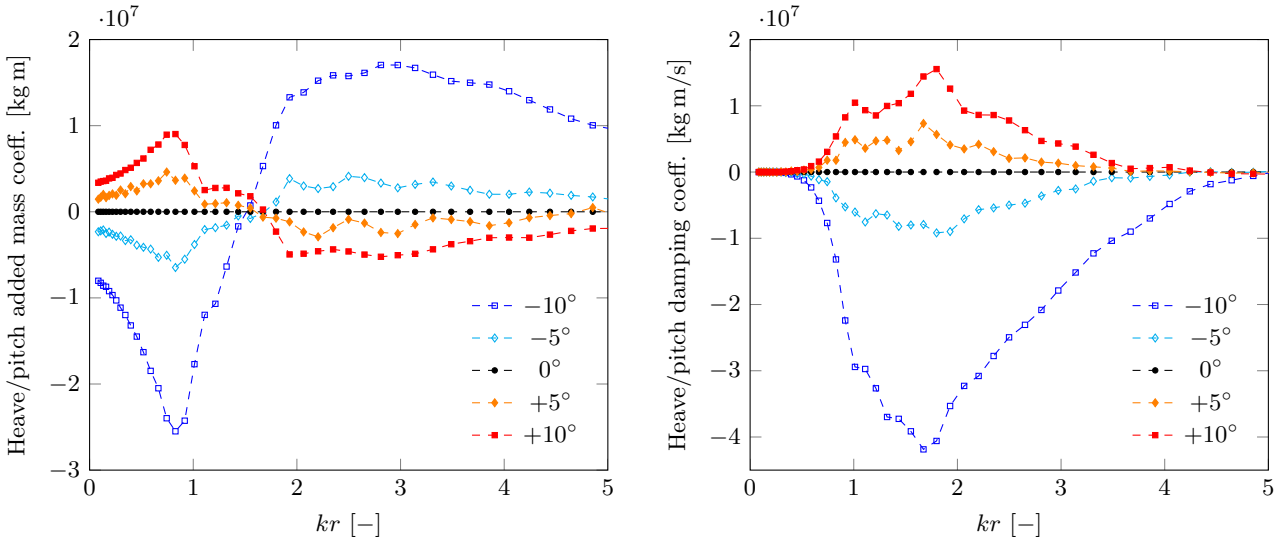

Figure 12: Inclination effects on the modified Dutch Tri-floater's heave-pitch coupling added mass and wave damping.

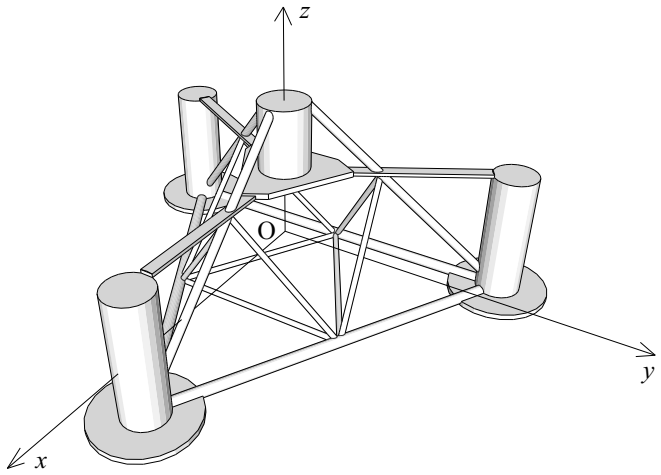

Figure 9: Modified Dutch Tri-floater geometry and system of reference.

Table 1: Modified Dutch Tri-floater geometric parameters.

Design draft [m]	12.0
Hull volume at design draft [m^3]	3048
Column centre-to-centre spacing [m]	68.0
Column diameter [m]	8.0
Column depth incl. plate [m]	24.0
Plate diameter [m]	18.0
Plate thickness [m]	1.0
Bracing diameter [m]	1.0 to 2.0

Table 2: Modified Dutch Tri-floater mass properties. Quantities are expressed with respect to the origin O at SWL.

Mass [t]	2263
Vertical position of CoG [m]	-0.1
Roll/pitch moment of inertia [t m^2]	$1.535 \cdot 10^6$
Yaw moment of inertia [t m^2]	$2.522 \cdot 10^6$

of the mean wetted surface enables to evaluate wave load variations via Nemoh. Water depth is assumed to equal 50 m, allowing to relate these results to the loading case of Section 3, and the chosen direction of propagation of the incident waves is along the x axis. The included graphs show the platform's vertical and vertical-rotational excitation features: Figure 10 displays the heave and pitch force response for the upright and trimmed configurations. It is possible to observe from the Figures that the imposed inclinations significantly modify wave excitation in the central portion of the studied range, which largely overlaps with the ocean wave band. For instance around $kr = 1.5$ (where the incident wave period is $T \approx 5$ s), an inclination of $+5\,^\circ$ practically doubles heave excitation and increases that of pitch by 30-50% compared to upright platform forces. Trimming also alters the radiation problem: while diagonal added masses are little impacted by trim-related excursion (cfr. 2.3), radiation damping is magnified by plate proximity to the surface as visible in Figure 11. Moreover, radiation-induced coupling appears in the trimmed configurations, due to the loss of hull axisymmetry. This is observable in Figure 12, where the introduction of heave-pitch hydrodynamic coupling is evidenced by the appearance of significant extra-diagonal terms. It is straightforward to relate the results of the current section to what presented in 2.3: reading the values of Figure 8 at the initial submergence of the platform plates, $s \approx 1.22$, helps to explain the divergence of the load response curves, which is most marked in the scattering parameter interval $kr \in [0.5, 4.0]$.

This section has shown that substantial changes of linear wave-structure interaction can occur when a semi-sub FWT platform equipped with water entrapment plates undergoes mean inclinations in the order of $5\,^\circ$ or more, un-

dermining validity of the classic small displacement assumption of wave load assessment. The following section presents a simple dynamic response analysis of the fully assembled turbine subject to wind and wave loading, aimed at evaluating the impact of the examined geometric nonlinearity on global FWT motion.

3. Dynamic response of a trimmed semi-sub floating wind turbine

Do the hydrodynamic effects explained in Section 2 significantly affect FWT motion in the presence of realistic wind and waves? A first-stage answer is here produced via frequency-domain dynamic response analysis of a moored modified Dutch Tri-floater platform supporting a NREL 5 MW reference turbine, detailed in Jonkman et al. (2009).

3.1. Methodology

The six-element vector containing the position of the FWT is defined as $\mathbf{x}$, where displacements are expressed in m and rotations in rad. Forces and moments are expressed in N and Nm respectively. In order to isolate potential hydrodynamic effects, all terms entering the 6-DoF frequency-domain equations of motion maintain the classic linearisation about the undisplaced, untrimmed position, with the exception of those derived from the BEM calculation. These consist of:

- Structural mass and inertia matrix $\mathbf{A}$, obtained by component assembly. It includes product inertias if $z_G \neq 0$.
- Linearised viscous damping matrix $\mathbf{B_v}$, iteratively obtained from a corresponding quadratic term (cfr. Equation 4).
- Hydrostatic stiffness matrix $\mathbf{C_h}$. Its computation includes the stabilising effect of mooring weight, that is lumped at the fairlead points located at plate centre, $z = -12$ m.
- Mooring stiffness matrix $\mathbf{C_m}$, supplied by Philippe (2012).

The inclination-dependent potential hydrodynamic terms are calculated ignoring all slender platform interconnectors. These are the added mass matrix $\mathbf{A_r}$, the wave damping matrix $\mathbf{B_r}$, and the hydrodynamic excitation vector $\mathbf{f_h}$. All mentioned quantities are expressed at the structure's waterplane centre O, the point of choice for resolution of rigid body dynamics. Rotor torque and gyroscopic effects are neglected. Steady wind excitation in the positive x direction takes the RHS form of

$$\mathbf{f_w}(\theta) = \begin{pmatrix} F_w \cos\theta & 0 & 0 & 0 & M_w \cos^2\theta & 0 \end{pmatrix}^{\mathrm{T}}, \quad (1)$$

where F_w is the sum of the rated thrust exerted on the untilted rotor and the tower's drag force, and M_w the related total overturning moment. θ denotes the FWT's trim angle about the y axis. The wind forces exerted on the floater's superstructures are neglected.

The structure's position under steady wind loading $\mathbf{x_0}$ is found by iteratively resolving the static equilibrium equation

$$\mathbf{x_0} = (\mathbf{C_h} + \mathbf{C_m})^{-1}\, \mathbf{f_w}(\mathbf{x_0}). \quad (2)$$

Following, wind forces are decoupled from displacement and the frequency domain equations of complex motion $\mathbf{x}$ about the mean equilibrium position found with Equation 2 are solved in the classic harmonic form:

$$\mathbf{x} = [-\omega^2(\mathbf{A} + \mathbf{A_r}) + i\omega(\mathbf{B_r} + \mathbf{B_v}) + (\mathbf{C_h} + \mathbf{C_m})]^{-1}\mathbf{f_h}. \quad (3)$$

As anticipated, presence of a linearised viscous term requires iterative resolution of the EoM, with the generalised n^{th} guess of the viscous damping matrix expressed by

$$\mathbf{B_v}^{(n)} = \frac{8}{3\pi}\mathbf{D_v}\,\omega\,|\mathbf{x}^{(n-1)}|, \quad (4)$$

where $\mathbf{D_v}$ is the constant quadratic drag matrix and $|\mathbf{x}^{(n-1)}|$ the element-by-element absolute value of the motion vector issued by the previous guess. $\mathbf{D_v}$ is obtained by integrating the maximum per-unit-velocity drag acting on all wetted members, including platform bracings and plates, when the structure undergoes small oscillations in still water. The transverse component of said drag force (i.e. normal to a cylinder's axis) is obtained by isolating the transverse component of the local velocity vector. The axial component of local drag - calculated for plates only - derives from the axial component of the velocity vector at plate centre. The dominating calibration parameter for the obtention of this term is the normal-flow heave plate drag coefficient, that has been set to 4.80 in analogy with that of a circular heave tank of similar size (see Masciola et al., 2013).

3.2. Definition of case study

The modified Dutch Tri-floater, detailed in 2.4.1, is assembled with the NREL 5 MW reference offshore wind turbine. The aerogenerator's tower has been adapted by Philippe (2012) to match the Dutch Tri-floater's central pylon height and diameter. A sketch of the FWT assembly is given in Figure 13, while the main particulars of the aerogenerator are available in Table 3. The FWT's mooring system is designed for 50 m water depth and consists in a three-line catenary arrangement. Its total weight in water equals 183.5 t and the linearised mooring stiffness matrix descending from quasi-static modelling is

$$\mathbf{C_m} = \begin{pmatrix} 1.6{\cdot}10^5 & 0 & 0 & 0 & 1.9{\cdot}10^6 & 0 \\ 0 & 1.6{\cdot}10^5 & 0 & -1.9{\cdot}10^6 & 0 & 0 \\ 0 & 0 & 1.5{\cdot}10^5 & 0 & 0 & 0 \\ 0 & -1.9{\cdot}10^6 & 0 & 1.1{\cdot}10^8 & 0 & 0 \\ 1.9{\cdot}10^6 & 0 & 0 & 0 & 1.1{\cdot}10^8 & 0 \\ 0 & 0 & 0 & 0 & 0 & 1.7{\cdot}10^8 \end{pmatrix}, \quad (5)$$

where the units are consistent with the definitions given in 3.1. The water depth specified above is also used in the diffraction/radiation model for consistency. The proposed loading case combines a steady rated wind of 11.4 m/s directed in the positive x direction with collinear regular waves of 4 m height.

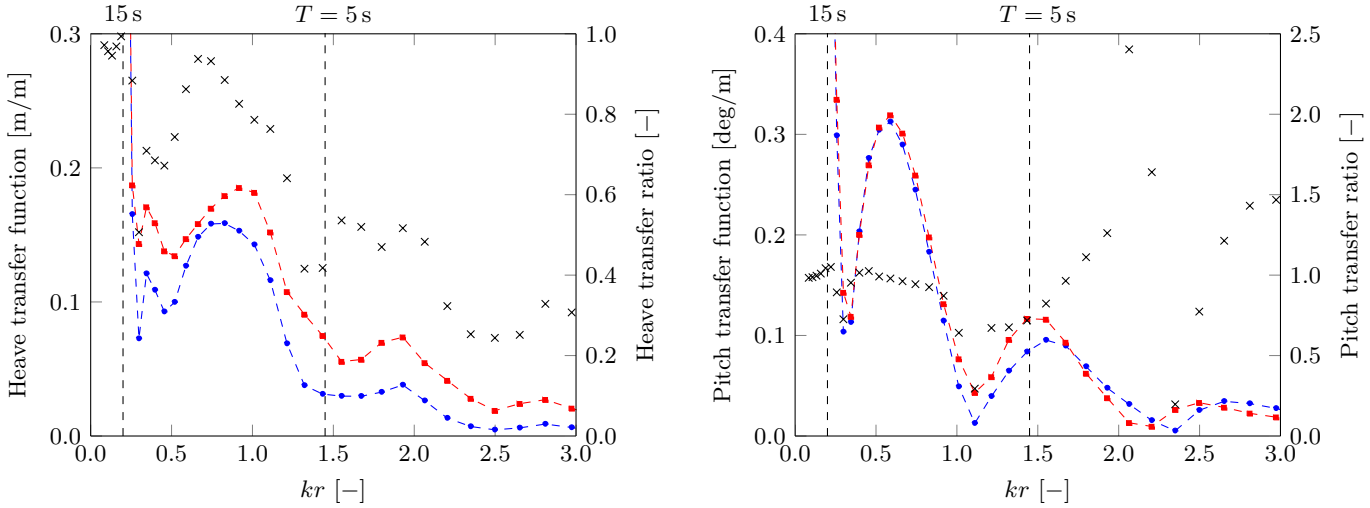

Figure 15: Case study turbine's heave and pitch response under collinear wind and wave excitation, using upright (blue dots) and inclined (red squares) wetted surface mesh. Crosses indicate the ratio between the two transfer functions.

Table 3: Adapted 3-blade upwind 5 MW NREL offshore wind turbine data. Quantities are expressed with respect to the origin O at SWL.

Mass [t]	678
Vertical position of CoG [m]	83.0
Roll/pitch moment of inertia $I_{xx} \approx I_{yy}$ [t m^2]	$3.779 \cdot 10^6$
Yaw moment of inertia [t m^2]	$5.220 \cdot 10^3$
Elevation of tower/floater interface [m]	25.0
Rotor diameter [m]	126
Rated wind speed [m/s]	11.4
Rated rotor thrust [kN]	810
Hub height [m]	90.0
Rated tower drag [kN]	43
Tower centre of pressure height [m]	54.8

3.3. Results

The mean equilibrium position found with Equation 2 consists of an offset of 4.05 m in the x direction and a trim about the y axis of 6.0 °, implying plate mean submergence to reach $s \approx 1.68$ (fore) and $s \approx 0.99$ (aft). The potential hydrodynamic database is calculated twice: once for zero trim and once for 6.0 °, whose actualised mesh is shown in Figure 14; the respective frequency-domain heave and pitch responses of the turbine are reported next. Plot ordinates are scaled so as to concentrate on the FWT response features in the 5 s to 15 s band. Figure 15 shows the calculated heave and pitch response when potential hydrodynamics are solved with and without the actualisation of the wetted surface.

The effect of increased vertical excitation clearly emerges from the heave response plot, and is easily related to the plate excursion effect of Figures 5 and 10. Motion in the $T \in [5\,\mathrm{s}, 15\,\mathrm{s}]$ interval, the main wave energy band, is always underestimated by the conventional potential approach, from 10% up to about 60% at the low period end of the interval. Moreover, the response suppression predicted by the conventional approach at $kr \approx 0.3$ ($T = 12$ s) is no longer found when inclination is accounted for. Added-mass-induced heave-pitch coupling that is only revealed by the actualisation approach also causes a slight increase in heave response in correspondence with pitch motion resonance, sited at a period above 15 s (cfr. Figure 12). Whilst not severe for the modified Dutch Tri-floater, this coupling effect may play a greater role in more compact FWT arrangements, whose heave/pitch modes lie closer to or within the wave band.

Pitch response is altered as well by the effect of integrating dynamic pressure on the actualised geometry, as visible in Figure 15. Within the 5 s to 15 s period interval, overlooking the effect of FWT inclinations causes a response underprediction of typically 30% at low periods; response suppression at $kr \approx 1.1$ also becomes less marked.

4. Discussion

The interaction of an underwater structure with surface waves is stronger when its submergence is small relative to its size. For a horizontal disc-shaped appendix, surface proximity effects are shown to significantly affect wave diffraction and radiation when its radius has the same order of magnitude as its draft or less, a condition that frequently holds for semi-submersible FWT water entrapment devices.

In the mathematical representation of linear water waves, the frequency-dependent exponential decay of diffraction and radiation potential in the vertical direction determines the existence of a certain plate excursion range where a small draft perturbation triggers large changes in wave patterns, and hence the related dynamic pressures and forces. In a semi-sub platform undergoing wind-induced trimming, heave plates appear to sweep such excursion

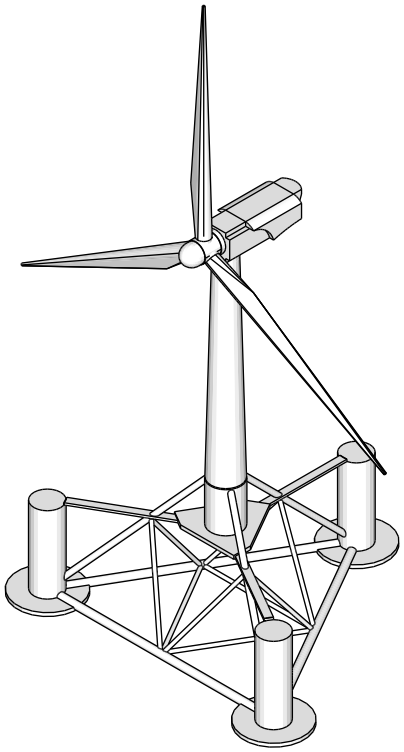

Figure 13: Modified Dutch Tri-floater with 5 MW class horizontal axis wind turbine. The depicted HAWT is an artist's impression adapted from a graphical model made available by Somerville (2014).

range for wave harmonics which are dominant in real sea spectra. Mean inclinations in the order of 5 ° cause enough hydrodynamic perturbation to significantly alter heave and pitch response, and to onset a heave-pitch coupling effect due to loss of radiation axisymmetry. Moreover, if one considers the maximum instantaneous inclinations reached under the combination of static and dynamic response (due to waves, but also wind gusts, etc.), said effects may undergo additional momentaneous magnification. In the chosen case study, pitch motion results less sensitive than heave to variable plate submergence. However, this may not hold for other semi-submersible FWT designs featuring lower pitch natural periods and/or larger pitch response in the ocean wave band.
The hydrodynamic effects discussed above are uncovered thanks to a mesh-updated linear potential method: the traditional method neglecting the mean displacement of the wetted surface is unable to capture such phenomena. The inclusion of inclination effects can improve the understanding of the FWT design constraints affecting the balance between static and dynamic response control.
Not treated in this work is the alteration of horizontal excitation and the appearance of horizontal-vertical coupling arising from trim. Furthermore, out-of-plane excitation and response are expected to occur when the inclination takes place about an axis different from pitch, or when waves and wind are not aligned: in these conditions the hull's remaining planar symmetry - conserved here about

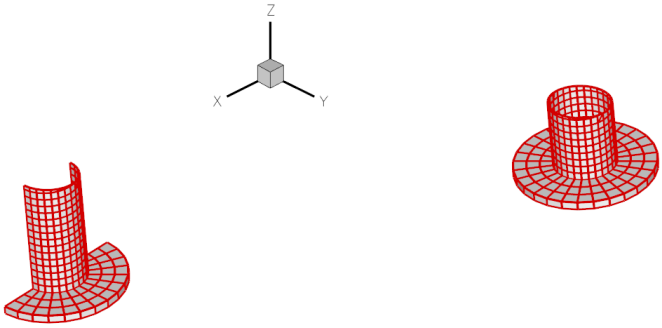

Figure 14: Actualised mesh of modified Dutch Tri-floater large members, with a 6.0 ° trim. Only half the structure is represented since the BEM solver can exploit planar symmetry to reduce problem size.

xz - is also lost, which brings in lateral excitation and additional coupling. All of the above cases can be analysed with the method presented here.
It is arguable that viscous hydrodynamic forces can also be significantly altered by FWT inclinations: the presence of relatively small-diameter hull members and sharp-edged appendices suggests that drag forces may play an important role in a certain band; the vertical excursion of the plates can possibly expose them to wave-induced drag regimes which strongly depend on the inclination of the FWT.
Finally, additional non-linear effects which are disregarded in this study are expected to become important as the plates approach the surface more closely, and in general for high-slope waves and/or large motion. Wave breaking, decomposition, and enhanced run-up above the plates may substantially alter the FWT loading regime and should be further studied in their impact on the turbine's loading and motion. At such levels of complexity linear potential theory needs to be replaced by higher order resolution of wave dynamics or a fully viscous representation.

5. Conclusions and further work

This study has shown the importance of including the heave plate excursion effects deriving from wind-induced inclination, and the subsequent geometric non-linearity, in dynamic response assessment of a semi-submersible FWT. In Section 2 the available literature covering the dependence of the wave forces exerted on a horizontal structure from its proximity to the free surface has allowed to outline the behaviour of an isolated heave plate in this context. Hence the linear potential BEM method, first applied on a surface-piercing column with bottom plate, and then on a trimming FWT platform, has shown their sensitivity to said submergence effects. A subsequent frequency-domain dynamic response analysis of a FWT under combined wind and wave loading has been organised in Section 3. This has shown that inclusion of plate excursion effects is required to correctly predict the turbine's response in the dominant ocean wave band, as discussed in Section 4. The use of

more advanced dynamic simulation methods may enable to evidence further impacts of wind-driven plate excursion on the motion of semi-submersible FWTs.

Acknowledgements

The authors are grateful for the funding provided by the ETI and the EPSRC RCUK Energy programme, and to EDF R&D for hosting and supervising the industrial doctorate.

References

Cermelli, C. A., Jul. 2014. Wind turbines ride the wave to renewable energy future. Online: http://www.gabreport.com/2012/08/wind-turbines-ride-the-wave-to-renewable-energy-future.

Cermelli, C. A., Roddier, D. G., 2005. Experimental and numerical investigation of the stabilizing effects of a water-entrapment plate on a deepwater minimal floating platform. In: Proc. 24th International Conference on Offshore Mechanics and Arctic Engineering. Halkidiki, Greece.

Courbois, A., Apr. 2013. Etude expérimentale du comportement dynamique d'une éolienne offshore flottante soumise à l'action conjuguée de la houle et du vent. Ph.D. thesis, Ecole Centrale de Nantes, Nantes, France.

ECN, Jun. 2014. LHEEA - nemoh. Online: http://lheea.ec-nantes.fr/doku.php/emo/nemoh/start.

EWEA, Jul. 2013. Deep water. the next step for offshore wind energy. Tech. rep., European Wind Energy Association.

Hitachi, 2014. The wind from the future - fukushima floating offshore wind farm demonstration project. Hitachi Review 63 (03), 12–17.

Hujis, F., Mikx, J., Savenije, F., de Ridder, E.-J., Nov. 2013. Integrated design of floater, mooring and control system for a semi-submersible floating wind turbine. Tech. rep.

IWES, May 2014. Industrialization setup of a floating offshore wind turbine. Online: http://www.inflow-fp7.eu/.

Jeon, S. H., Cho, Y. U., Seo, M. W., Cho, J. R., Jeong, W. B., Nov. 2013. Dynamic response of floating substructure of spar-type offshore wind turbine with catenary mooring cables. Ocean Engineering 72, 356–364.

Jonkman, J., Butterfield, S., Musial, W., Scott, G., Feb. 2009. Definition of a 5 MW reference wind turbine for offshore system development. Tech. Rep. NREL/TP-500-38060, National Renewable Energy Laboratory.

Journée, J. M. J., Massie, W. W., 2000. Offshore Hydromechanics. TU Delft, Delft, The Netherlands.

Karimirad, M., Moan, T., Jul. 2012. A simplified method for coupled analysis of floating offshore wind turbines. Marine Structures 27 (1), 45–63.

Kojima, H., Ijima, T., Yoshida, A., 1990. Decomposition and interception of long waves by a submerged horizontal plate. In: Proc. 22nd Conference on Coastal Engineering. Delft, The Netherlands, pp. 1228–1241.

Kojima, H., Yoshida, A., Nakamura, T., 1994. Linear and nonlinear wave forces exerted on a submerged horizontal plate. Coastal Engineering 1 (24), 1312–1326.

Lake, M., He, H., Troesch, A. W., Perlin, M., Thiagarajan, K. P., 2000. Hydrodynamic coefficient estimation for TLP and spar structures. Journal of Offshore Mechanics and Arctic Engineering 122 (2), 118.

Lamb, H., Jun. 1945. Hydrodynamics, 6th Edition. Dover Publications, New York, USA.

Linton, C. M., Evans, D. V., 1991. Trapped modes above a submerged horizontal plate. The Quarterly Journal of Mechanics and Applied Mathematics 44 (3), 487–506.

Maciel, J. G., Oct. 2012. The WindFloat project. Presentation at the Conference Atlantic Forum 2012, Brest, France.

Main(e) IC, May 2013. Floating offshore wind foundations: Industry consortia and projects in the united states, europe and japan. Tech. rep., Main(e) International Consulting LLC.

Martin, P. A., Farina, L., 1997. Radiation of water waves by a heaving submerged horizontal disc. Journal of Fluid Mechanics 337, 365–379.

Masciola, M., Robertson, A., Jonkman, J., Coulling, A., Goupee, A., 2013. Assessment of the importance of mooring dynamics on the global response of the deepcwind floating semisubmersible offshore wind turbine. In: Proc. 23rd International Offshore and Polar Engineering Conference. Anchorage, Alaska, USA.

McIver, M., 1985. Diffraction of water waves by a moored, horizontal, flat plate. Journal of Engineering Mathematics 19 (4), 297–319.

Nénuphar, Oct. 2012. Vertiwind: making floating wind turbine technology competitive for offshore. Presentation. Online: http://www.twenties-project.eu/system/files/2_2013-03%20Presentation%20short.pdf.

Parsons, N. F., Martin, P. A., 1995. Trapping of water waves by submerged plates using hypersingular integral equations. Journal of Fluid Mechanics 284, 359–375.

Philippe, M., Oct. 2012. Couplages aéro-hydrodynamiques pour l'étude de la tenue à la mer des éoliennes offshore flottantes. Ph.D. thesis, Ecole Centrale de Nantes, Nantes, France.

Philippe, M., Babarit, A., Ferrant, P., Jan. 2013a. Modes of response of an offshore wind turbine with directional wind and waves. Renewable Energy 49, 151–155.

Philippe, M., Courbois, A., Babarit, A., Bonnefoy, F., Rousset, J.-M., Ferrant, P., 2013b. Comparison of simulation and tank test results of a semi-submersible floating wind turbine under wind and wave loads. In: Proc. 32nd International Conference on Ocean, Offshore and Arctic Engineering. American Society of Mechanical Engineers, Nantes, France.

Porter, R., 2014. Linearised water wave problems involving submerged horizontal plates. Applied Ocean Research (in press).

Scott, A., May 2012. The ETI's floating offshore wind demonstrator. Presentation at All Energy 2012, Aberdeen, Scotland, UK.

Sethuraman, L., Venugopal, V., Apr. 2013. Hydrodynamic response of a stepped-spar floating wind turbine: Numerical modelling and tank testing. Renewable Energy 52, 160–174.

Somerville, M., Jun. 2014. GE 3.6 MW offshore wind turbine - 3d warehouse. Online: https://3dwarehouse.sketchup.com.

Stiesdal, H., Dec. 2009. Hywind: The world's first floating MW-scale wind turbine. Wind Directions, 52–53.

Tao, L., Cai, S., 2004. Heave motion suppression of a spar with a heave plate. Ocean Engineering 31 (5), 669–692.

Tao, L., Molin, B., Scolan, Y. M., Thiagarajan, K., Nov. 2007. Spacing effects on hydrodynamics of heave plates on offshore structures. Journal of Fluids and Structures 23 (8), 1119–1136.

Thiagarajan, K. P., Datta, I., Ran, A. Z., Tao, L., Halkyard, J. E., 2002. Influence of heave plate geometry on the heave response of classic spars. In: Proc. 21st International Conference on Offshore Mechanics and Arctic Engineering. Oslo, Norway, p. 621–627.

Vada, T., 1987. A numerical solution of the second-order wave-diffraction problem for a submerged cylinder of arbitrary shape. Journal of Fluid Mechanics 174, 23–37.

Wang, L., Sweetman, B., Oct. 2013. Multibody dynamics of floating wind turbines with large-amplitude motion. Applied Ocean Research 43, 1–10.

Yu, X., 2002. Functional performance of a submerged and essentially horizontal plate for offshore wave control: a review. Coastal Engineering Journal 44 (02), 127–147.

Yu, X., Dong, Z., Sep. 2001. Direct computation of wave motion around submerged plates. In: Proc. 29th International Association for Hydro-Environment Engineering and Research. Beijing, China.

Yu, X., Isobe, M., Watanabe, A., 1995. Wave breaking over submerged horizontal plate. Journal of Waterway, Port, Coastal, and Ocean Engineering 121 (2), 105–113.

Zheng, Y. H., Liu, P. F., Shen, Y. M., Wu, B. J., Sheng, S. W., Mar. 2007. On the radiation and diffraction of linear water waves by an infinitely long rectangular structure submerged in oblique seas. Ocean Engineering 34 (3–4), 436–450.